AIAA JOURNAL
Vol. 38, No. 5, May 2000

Multiple Inviscid Solutions for the Flow in a Leading-Edge Vortex

M. B. H. van Noordenburg* and H. W. M. Hoeijmakers†
University of Twente, 7500 AE Enschede, The Netherlands

To analyze the flowfield inside the vortex formed at the leading edge of a highly swept wing at an angle of attack, conical similarity solutions of the compressible Euler equations have been obtained and compared to incompressible conical similarity flow solutions. It is shown that, in contrast to the incompressible flow case, the velocity components inside the vortex core remain finite in the interior of the vortex. The compressible and inviscid flow solution exhibits vacuum conditions at the axis of the vortex core. Two different families of solutions have been numerically obtained, one representing jetlike swirling flow solutions and the other wakelike swirling flow solutions. Considering the flow solutions in more detail reveals that, at the edge of the vortex core, the normal component of the velocity is negative (inflow) for jetlike swirling flows and positive (outflow) for wakelike swirling flows. The velocity and the vorticity vector are parallel for jetlike swirling flows and antiparallel for wakelike swirling flows. Furthermore, the azimuthal component of the vorticity has a different direction for both flow solutions. Varying the boundary conditions, for instance, the swirl number or the Mach number, at the edge of the vortex core does not change the character of the flow solutions significantly.

Nomenclature

$\boldsymbol{E}$	= functional
H	= total enthalpy
p	= pressure
$R(x)$	= local radius of vortex core
R'	= tangent of semivertex angle of the vortex core
u_r, u_x, u_ϕ	= velocity components in cylindrical coordinate system
$\boldsymbol{X}$	= state vector
x, r, ϕ	= cylindrical coordinate system
Γ	= circulation
γ	= ratio of specific heats in free air
κ	= constant
ρ	= density
ρ_∞	= freestream density
$\omega_x, \omega_r, \omega_\phi$	= vorticity components in cylindrical coordinate system

I. Introduction

IN the case of the flow around airplanes with a highly swept wing at incidence, military aircraft, for instance, boundary-layer separation at the leading edge of the wings leads to the formation of vortical structures formed by the rolling up of the shear layers. Such vortical structures, called vortices for short, consist of regions of concentrated vorticity. The concentration of vorticity in elongated regions of relatively small cross section counteracts the influence of dissipative processes. These vortical structures remain, therefore, fairly coherent and persistent. They can persist for miles downstream of an airplane. The vortices formed at the leading edge of highly swept wings and located above the wing upper surface induce an additional so-called vortex-induced lift force that enables flight at higher angles of attack than without leading-edge flow separation in a controllable manner. Above a critical angle of attack, however, the internal structure of the leading-edge vortex changes dramatically, resulting in an abrupt increase in the cross-sectional size of the vortex. The leading-edge vortex loses its compact and coherent structure, thereby significantly increasing the influences of dissipative processes. This phenomenon is called vortex breakdown or vortex burst and signifies the end of the favorable effects of the leading-edge vortex, for example, the end of the additional lift force.

Examination of measurements of the flow inside the leading-edge vortex reveals that the leading-edge vortex can be described by the distinguishing of three separate regions: the outer shear layer, an inviscid vortex core, and a viscous subcore.[1] The vortex core seems to be fairly axisymmetric and grows linearly in downstream direction thereby forming a conical flow region.[2–4] The cross-sectional size of the vortex core is found to be effectively independent of the Reynolds number. Examining the measured flowfield inside the leading-edge vortex core at different downstream locations indicates that the flowfield inside the vortex core is nearly conical, at least for the initial part of the vortex (e.g., see Refs. 2 and 4). Furthermore, the circulation grows linearly in the downstream direction. The flowfield surrounding the leading-edge vortex core is, however, a complex three-dimensional unsteady flowfield.

Based on these experimental observations, in the past decades a large number of researchers have tried to model the flow inside the leading-edge vortex core. Almost all of the models of the leading-edge vortex assume that the vortex is axisymmetric and that it is possible to consider an isolated vortex core, that is, in isolation from natural surroundings, by representing the external influence onto the vortex core through boundary conditions. The leading-edge vortex is rather slender and grows linearly in the downstream direction. Based on these observations, a conical similarity solution has been obtained by Hall[5] and Ludwieg[6] for incompressible and inviscid flow inside a vortex core. For the outer part of the vortex core, this solution qualitatively resembles the flow inside a leading-edge vortex. At the axis of the core, however, this solution possesses a logarithmic singularity for the axial and azimuthal component of the velocity rendering the solution non-physical. This inviscid solution was extended by Stewartson and Hall[7] by matching the inviscid conical outer solution to a viscous subcore through an asymptotic analysis. In this way the logarithmic singularities were removed at the axis of the vortex core. Brown[8] added the effect of compressibility to Hall's solution.[5] Brown[8] obtained a compressible and inviscid conical similarity solution without the logarithmic singularity that was obtained by Hall.[5] However, removing the logarithmic singularity from the flowfield resulted in reaching vacuum conditions at the axis of the vortex core. Recently Mayer and Powell[9] included the influence of viscosity to the flow in the interior of the leading-edge vortex to demonstrate that adding viscosity to the flow prevents the solution from reaching vacuum conditions at the axis of the core.

Hoeijmakers[10] used the axisymmetric form of the incompressible Euler equations to obtain analytically two conical similarity

Received 19 October 1998; revision received 16 July 1999; accepted for publication 3 September 1999.

*Ph.D. Student, P.O. Box 217, Department of Mechanical Engineering. Student Member AIAA.

†Professor, P.O. Box 217, Department of Mechanical Engineering. Senior Member AIAA.

solutions for identical boundary conditions: one solution being the one already obtained by Hall[5] for slender vortices and the second one a completely different solution. The existence of multiple flow solutions satisfying identical boundary conditions could indicate that vortex breakdown may be related to a jump between different steady-state flow solutions of the governing equations. The dynamics of this jump might already be present in the inviscid Euler equations. The hypothesis that the breakdown phenomenon might be a transition between two steady flow states had already been proposed by Benjamin[11] in the early 1960s. In the remainder of the present study the inviscid Euler equations (both incompressible and compressible) are assumed to possess conical similarity flow solutions for the flow inside the leading-edge vortex core. First, the incompressible flow solutions (already obtained by Hoeijmakers[10]) are investigated, and specific features of the flow solutions are considered in more detail. Second, the influence of compressibility on the flow solutions and the possible existence of multiple compressible flow solutions satisfying identical boundary conditions are addressed. The existence of multiple similarity solutions with different flow characteristics might be used in the development of simple methods to predict the occurrence of breakdown or they may be used as input parameters for more advanced methods to describe the flow inside the leading-edge vortex, such as variational methods (cf. Wang and Rusak[12]), parabolized Navier–Stokes equations (cf. Berger and Erlebacher[13]) or direct numerical simulation (cf. Visbal[3]).

II. Basic Equations

The leading-edge vortex appears to be fairly axisymmetric and to consist of an inviscid rotational outer core and a viscid subcore. In the present investigation it is assumed that the effects of viscosity on the flow inside the leading-edge vortex core can be neglected. Of course, at the axis of the vortex core this will result in an unrealistic flowfield, but it is assumed that the outer part of the vortex core will be properly described. To describe the flowfield inside the leading-edge vortex, the axisymmetric form of the Euler equations is used:

$$\frac{\partial\rho}{\partial t}+\frac{\partial\rho u_x}{\partial x}+\frac{\partial\rho u_r}{\partial r}+\frac{\rho u_r}{r}=0$$

$$\frac{\partial u_x}{\partial t}+u_x\frac{\partial u_x}{\partial x}+u_r\frac{\partial u_x}{\partial r}=-\frac{1}{\rho}\frac{\partial p}{\partial x}$$

$$\frac{\partial u_r}{\partial t}+u_x\frac{\partial u_r}{\partial x}+u_r\frac{\partial u_r}{\partial r}-\frac{u_\phi^2}{r}=-\frac{1}{\rho}\frac{\partial p}{\partial r}$$

$$\frac{\partial u_\phi}{\partial t}+u_x\frac{\partial u_\phi}{\partial x}+u_r\frac{\partial u_\phi}{\partial r}+\frac{u_r u_\phi}{r}=0 \tag{1}$$

where x is the coordinate along the axis of the vortex core and r the radial distance to the axis of the core. In the case of incompressible flow ($\rho=\rho_\infty$), Eq. (1) can be solved for u_x, u_r, u_ϕ, and p. In case of compressible flow, we have to add the energy equation and the equations of state to complete the system of equations. From experimental observations it follows that above the wing the leading-edge vortex has a conical shape. To analyze the axisymmetric form of the Euler equations, therefore, a useful coordinate transformation is

$$z=x, \qquad \sigma=r/R(x)$$

By use of this coordinate transformation, the partial derivatives in the axisymmetric Euler equations become

$$\frac{\partial}{\partial r}=\frac{1}{R(z)}\frac{\partial}{\partial\sigma}, \qquad \frac{\partial}{\partial x}=\frac{\partial}{\partial z}-\frac{\sigma R'(z)}{R(z)}\frac{\partial}{\partial\sigma}$$

Substituting these relations in the Euler equations (1) leads to the following set of equations:

$$R(z)\frac{\partial\rho}{\partial t}-\sigma\frac{\partial\rho(R'u_x-u_r/\sigma)}{\partial\sigma}+\frac{2\rho u_r}{\sigma}=-R(z)\frac{\partial\rho u_x}{\partial z}$$

$$R(z)\frac{\partial u_x}{\partial t}-\sigma\left(R'u_x-\frac{u_r}{\sigma}\right)\frac{\partial u_x}{\partial\sigma}-R'\frac{\sigma}{\rho}\frac{\partial p}{\partial\sigma}=-R(z)\left(u_x\frac{\partial u_x}{\partial z}+\frac{1}{\rho}\frac{\partial p}{\partial z}\right)$$

$$R(z)\frac{\partial u_r}{\partial t}-\sigma\left(R'u_x-\frac{u_r}{\sigma}\right)\frac{\partial u_r}{\partial\sigma}+\frac{1}{\rho}\frac{\partial p}{\partial\sigma}-\frac{u_\phi^2}{\sigma}=-R(z)u_x\frac{\partial u_r}{\partial z}$$

$$R(z)\frac{\partial u_\phi}{\partial t}-\sigma\left(R'u_x-\frac{u_r}{\sigma}\right)\frac{\partial u_\phi}{\partial\sigma}+\frac{u_r u_\phi}{\sigma}=-R(z)u_x\frac{\partial u_\phi}{z} \tag{2}$$

where $R'(z)$ is the derivative of $R(z)$ with respect to z. For the conical flow case, $R'(z)$ will be a constant describing the slope of the vortex core.

The vorticity vector is given by $\boldsymbol{\omega}=\nabla\times\boldsymbol{u}$ that in cylindrical coordinates has the components

$$\omega_x=\frac{1}{r}\frac{\partial r u_\phi}{\partial r}-\frac{1}{r}\frac{\partial u_r}{\partial\phi}, \qquad \omega_r=\frac{1}{r}\frac{\partial u_x}{\partial\phi}-\frac{\partial u_\phi}{\partial x}$$

$$\omega_\phi=\frac{\partial u_r}{\partial x}-\frac{\partial u_x}{\partial r} \tag{3}$$

Thus, for the axisymmetric case we find in terms of σ and z

$$\omega_x=\frac{1}{\sigma R(z)}\frac{\partial\sigma u_\phi}{\partial\sigma}, \qquad \omega_r=\frac{\sigma R'(z)}{R(z)}\frac{\partial u_\phi}{\partial\sigma}-\frac{\partial u_\phi}{\partial z}$$

$$\omega_\phi=\frac{\partial u_r}{\partial z}-\frac{\sigma R'(z)}{R(z)}\frac{\partial u_r}{\partial\sigma}-\frac{1}{R(z)}\frac{\partial u_x}{\partial\sigma} \tag{4}$$

III. Incompressible Flow

Under the assumption that the flow in the vortex core is conical the partial derivatives with respect to z in Eqs. (2) drop out. Then assuming that the flow is steady and incompressible makes it possible to obtain an analytic solution for the remaining set of ordinary differential equations, that is,

$$-\sigma\frac{\mathrm{d}}{\mathrm{d}\sigma}\left(R'u_x-\frac{u_r}{\sigma}\right)+\frac{2u_r}{\sigma}=0$$

$$-\sigma\left(R'u_x-\frac{u_r}{\sigma}\right)\frac{\mathrm{d}u_x}{\mathrm{d}\sigma}-R'\frac{\sigma}{\rho_\infty}\frac{\mathrm{d}p}{\mathrm{d}\sigma}=0$$

$$-\sigma\left(R'u_x-\frac{u_r}{\sigma}\right)\frac{\mathrm{d}u_r}{\mathrm{d}\sigma}+\frac{1}{\rho_\infty}\frac{\mathrm{d}p}{\mathrm{d}\sigma}-\frac{u_\phi^2}{\sigma}=0$$

$$-\sigma\left(R'u_x-\frac{u_r}{\sigma}\right)\frac{\mathrm{d}u_\phi}{\mathrm{d}\sigma}+\frac{u_r u_\phi}{\sigma}=0 \tag{5}$$

where R' is a constant that represents the slope of the core. The appropriate boundary conditions for this problem are given by $u_r=0$ at $\sigma=0$, and the axial and circumferential components of the velocity as well as the pressure are specified at $\sigma=1$, that is, U_e, V_e, and P_e, respectively, at the edge of the core.

After some manipulation[10] one obtains the following two families of closed-form solutions of Eqs. (5):

$$u_x=U_e\left\{1-\alpha\ell n\left(\frac{G(\sigma)}{G(1)}\right)\right\}, \qquad u_r=-U_e\alpha G(\sigma)$$

$$u_\phi=V_e\left(1+\left(\frac{U_e\alpha}{V_e}\right)^2\left\{\frac{G(\sigma)}{\sigma R'}-\frac{G(1)}{R'}-\ell n\left(\frac{G(\sigma)}{G(1)}\right)\right\}\right)^{\frac{1}{2}}$$

$$\frac{p}{\rho_\infty}=\frac{P_e}{\rho_\infty}+V_e^2\left(\ell n\frac{G(\sigma)}{G(1)}+\frac{1}{2}\left(\frac{U_e\alpha}{V_e}\right)^2\left\{\frac{G(\sigma)}{\sigma R'}-\frac{G(1)}{R'}+G(1)^2\,\ell n\frac{G(\sigma)}{G(1)}-\left(\ell n\frac{G(\sigma)}{G(1)}\right)^2\right\}\right) \tag{6}$$

where

$$G(\sigma) = \frac{[1 + (\sigma R')^2]^{\frac{1}{2}} - 1}{\sigma R'} > 0$$

$$\alpha = \frac{\pm\left[1 + 4(V_e/U_e)^2 G(1)/R'\right]^{\frac{1}{2}} - 1}{2G(1)/R'}$$

Two distinct families of solutions are analytically obtained. The difference between the two solutions is governed by the parameter α. The parameter α is either positive or negative. For negative values of the parameter α, the flow solution represents a jetlike swirling flow, whereas for a positive value of α, a wakelike swirling flow is obtained. This means that, subject to identical boundary conditions at the edge of the vortex core, two different velocity and pressure distributions inside the core are obtained. It follows directly from the momentum equation that for incompressible steady flow the total enthalpy, defined as

$$H = p/\rho_\infty + \tfrac{1}{2}\left(u_x^2 + u_r^2 + u_\phi^2\right) \tag{7}$$

must be constant along streamlines. It can be shown that the total enthalpy for the two families of closed-form solutions is equal to

$$P_e/\rho_\infty + \tfrac{1}{2}\left[U_e^2 + V_e^2 + \alpha^2 G^2(1) U_e^2\right] \tag{8}$$

which is independent of the coordinate σ, that is, a constant, equal to the value of the total enthalpy at the edge of the vortex core. This implies that all streamlines intersect the edge of the vortex core. It immediately follows that the total enthalpy of one family of flow solutions is larger than that for the other family of flow solutions under identical boundary conditions (a larger value of α^2 while keeping all other parameters fixed).

In Fig. 1 the jetlike swirling flow is compared to the experimentally obtained velocity distributions inside a leading-edge vortex core generated above a 76-deg delta wing at 20.4-deg angle of attack at different locations along the root chord of the wing. For more detailed information about the experimental obtained velocity distributions refer to Verhaagen et al.[14] and Verhaagen et al.[15] For R' the value of 0.0625 is taken, and the swirl number, that is, V_e/U_e, is set to $\frac{10}{13}$. Note that the experimental obtained velocity distributions are scaled by the freestream axial velocity component and not by the axial velocity component at the edge of the vortex core. As a consequence, the scaled axial velocity component of the velocity is not equal to 1 at the edge of the vortex core. It is clear from Fig. 1 that outside a small region near the axis of the core the jetlike swirling flow solution is in qualitative agreement with experimental observations. At and near the axis of the vortex core, viscous effects become important. Furthermore, the velocity profile at different locations along the root chord of the wing indicates that the flowfield inside the leading-edge vortex core is fairly similar justifying the conical similarity assumption.

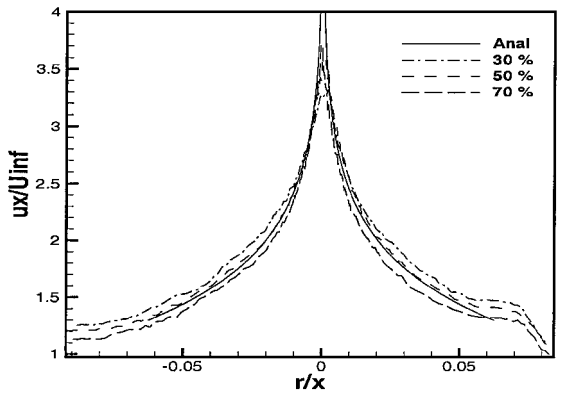

Axial

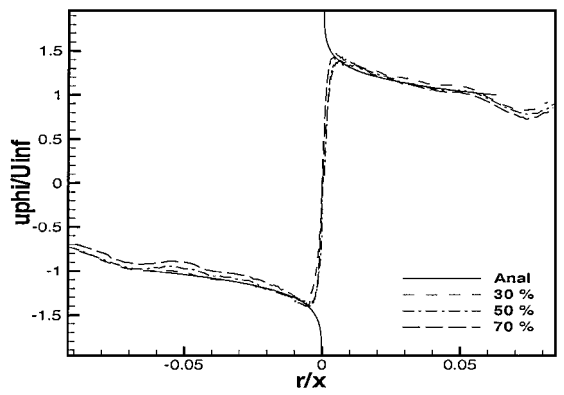

Azimuthal

Fig. 1 Experimentally obtained velocity distributions compared to conical similarity solution.

The shape of the velocity and pressure distributions for each family of conical similarity solutions only depends on the swirl number and on the tangent of the core half-angle R'. To facilitate the comparison of the two families of solutions, the velocity components and the dimensionless circulation $\Gamma/[2\pi R(z)U_e]$ inside the core are shown in Fig. 2 for various values of the swirl parameter. The slope of the vortex core is taken to be 0.0625. From Fig. 2 one sees that the most striking difference between the two families of solutions is that the first family of solutions represent a jetlike flow and the second family a wakelike flow. The jetlike flow solution has also been obtained by Hall[5] and Ludwieg[6] for slender vortices. Also, note that the radial component of the velocity has a different sign, and it can be verified that at the edge of the core the normal component of the velocity, that is, $(u_r - R'u_x)/\sqrt{[1 + (R')^2]}$, is negative (inflow) for the jetlike solution and positive (outflow) for the wakelike solution. The first family of solutions resembles the flow inside the leading-edge vortex core before vortex breakdown (see Fig. 1); the second family of solutions represents a completely different flow solution. Both solutions, however, are logarithmically singular at the axis of the core, which is of course physically not correct. By the examination of the analytic solutions at the center of the core, it follows that for $\sigma \to 0$ the pressure tends to infinity as $[\ell n(\sigma)]^2$, the axial component of the velocity as $-\ell n(\sigma)$, and the circumferential component as $[-\ell n(\sigma)]^{1/2}$. Clearly the effects of compressibility and viscosity cannot be neglected at and near the axis of the core because it is expected that at the axis the physically realistic compressible viscous flow solution will have a finite pressure and finite axial velocity, as well as zero azimuthal velocity. It is observed that the character of the solution does not change with the swirl parameter; specifically, for a swirl parameter around 1.0, which is believed to be a critical value for vortex breakdown, nothing remarkable occurs.

The vorticity distribution within the core can be obtained analytically from the velocity distribution, using Eqs. (4), as

$$\omega_x = \frac{V_e}{\sigma R(z)} \times \frac{1 - (U_e\alpha/V_e)^2\{G(1)/R' + \ell n[G(\sigma)/G(1)]\}}{1 + (U_e\alpha/V_e)^2\{G(\sigma)/\sigma R' - G(1)/R' - \ell n[G(\sigma)/G(1)]\}^{\frac{1}{2}}}$$

$$\omega_r = -\frac{V_e}{\sigma R(z)}\left(\frac{U_e\alpha}{V_e}\right)^2 \times \frac{G(\sigma)}{1 + (U_e\alpha/V_e)^2\{G(\sigma)/\sigma R' - G(1)/R' - \ell n[G(\sigma)/G(1)]\}^{\frac{1}{2}}}$$

$$\omega_\phi = \frac{V_e}{\sigma R(z)}\frac{U_e\alpha}{V_e} \tag{9}$$

From Crocco's law we find that for steady, isoenergetic, isentropic, and inviscid flows not subject to a volumetric force field the vorticity vector and the velocity vector should be parallel or antiparallel, that is,

$$\boldsymbol{u} \times \boldsymbol{\omega} = \boldsymbol{0} \tag{10}$$

The preceding obtained solutions indeed satisfy this relationship. The vorticity distribution for unit swirl number is shown in Fig. 3.

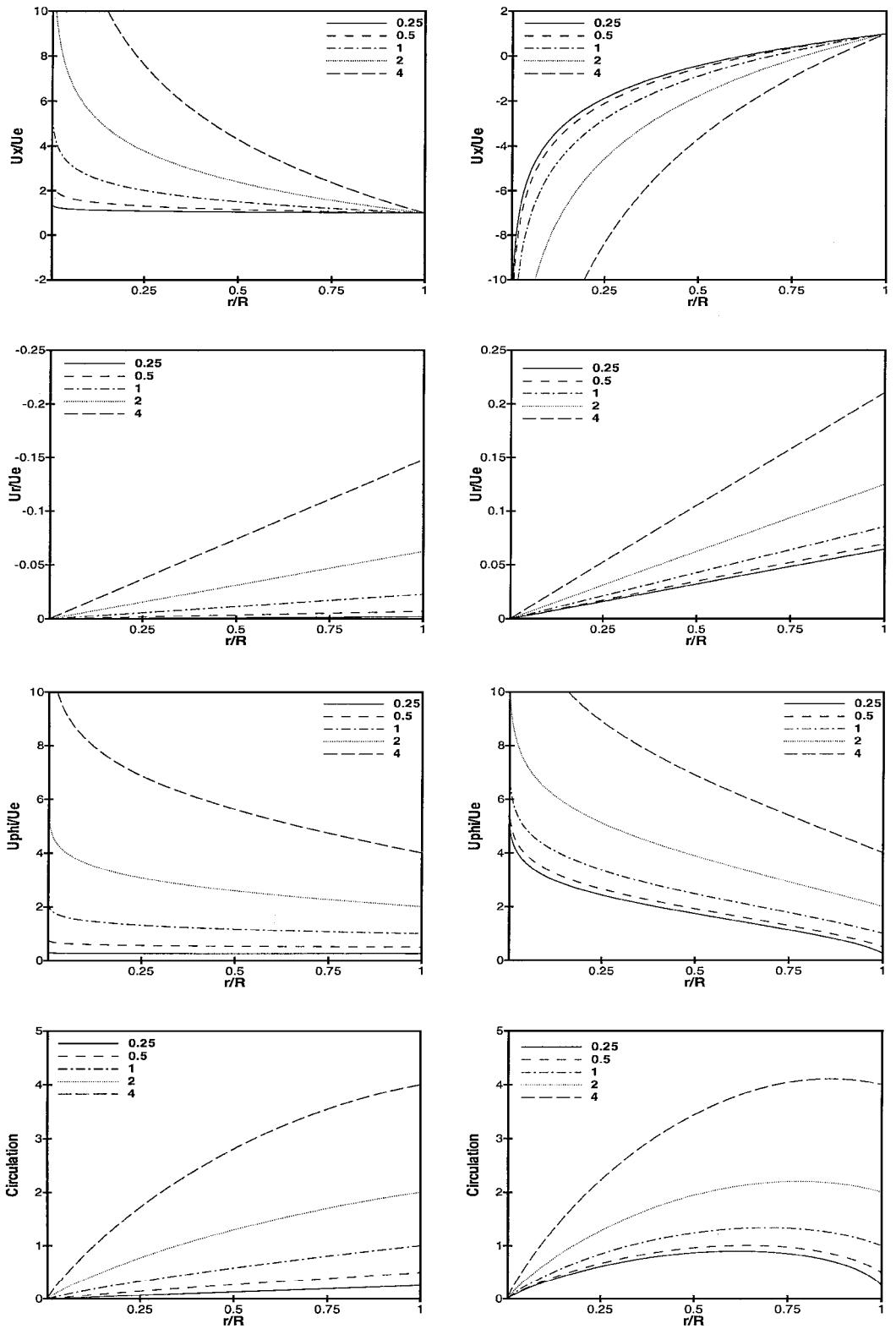

Fig. 2 Velocity components and the circulation for first (left) and second (right) family of solutions for various values of the swirl parameter V_e/U_e ($R' = 0.0625$); circulation is scaled by $2\pi RU_e$.

The most significant difference between the vorticity distributions associated with the two different families is present in the azimuthal component of the vorticity, which has a different sign. (Note that the scales of the two plots for the azimuthal component of vorticity in Fig. 3 are different.) In recent publications,[16,17] a switch in the sign of the azimuthal component of the vorticity has been identified as a key factor in the vortex breakdown phenomenon. The existence of two solutions under identical boundary conditions with a different direction of the azimuthal component of the vorticity could suggest that the vortex breakdown phenomenon might be a transition between steady-state flow solutions and might indicate that the inviscid Euler equations could be capable of capturing the main dynamics of this phenomenon, at least the initial part of this phenomenon. By the examination of expressions (9), it follows that $\omega_x \sim 1/\sigma(-\ell n\sigma)^{1/2}$ and $\omega_\phi \sim 1/\sigma$ for $\sigma \to 0$, that is, the vorticity distribution becomes, like the velocity distribution, singular at the axis of the core. This is clearly not physical and is due to the neglect of the effects of compressibility and viscosity. Also noteworthy is

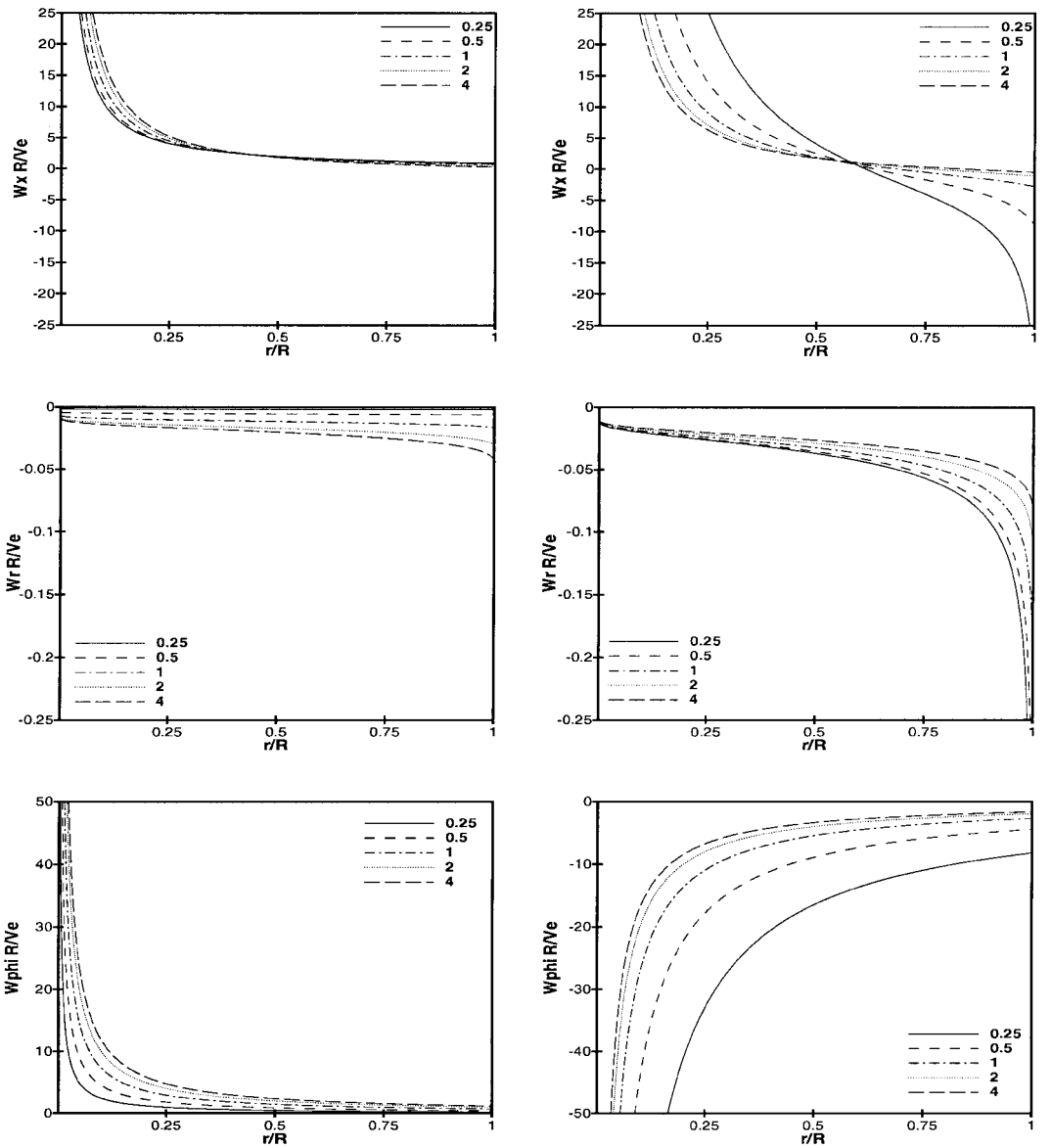

Fig. 3 Vorticity distribution inside the core for first (left) and second (right) family of solutions for various values of the swirl parameter V_e/U_e ($R' = 0.0625$).

that, in the wakelike type of solution, the axial component of the vorticity is negative in the region near the edge of the vortex, which is also evident from the circulation distribution that, for this family of solutions, has a maximum inside the core (see Fig. 2).

Furthermore, the normalized helicity density defined as

$$\frac{\boldsymbol{u} \cdot \boldsymbol{\omega}}{|\boldsymbol{u}| \cdot |\boldsymbol{\omega}|} \tag{11}$$

can be shown to be $+1$ for the jetlike solution and -1 for the wakelike solution, indicating that for the jetlike solution the velocity and vorticity vectors are pointing in the same direction, whereas for the wakelike solution the two vectors point in opposite directions. This means that while for the jetlike solution the streamlines are entering the core and for the wakelike solution the streamlines are leaving the domain, in both cases vorticity is entering the domain, in accordance with the boundary conditions, which imply that the circulation is increasing linearly with the coordinate along the x axis.

In Fig. 4 a three-dimensional view of a streamline that intersects the edge of the vortex core is given for both types of solutions. For the jetlike solution, the streamline enters the vortex core from an upstream location and continues downstream spiraling toward the axis of the core, whereas for the wakelike solution the streamline originates at a downstream location and moves upstream and away from the axis until the point where the axial component of the velocity becomes positive again. At this location the streamline starts to move in a downstream direction continuing to move toward the edge of the vortex core.

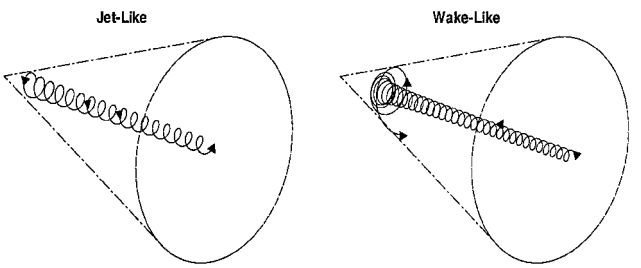

Fig. 4 Three-dimensional streamline for the jetlike solution (left) and wakelike solution (right) for swirl parameter V_e/U_e set to unity and $R' = 0.0625$.

IV. Compressible Flow

To obtain a more physical representation of the leading-edge vortex the effect of compressibility is to be included. Under the assumption that the flow in the vortex is conical, the partial derivatives with respect to z in Eqs. (2) drop out. We furthermore assume

that the flow in the vortex core is isentropic and that the gas satisfies the calorically perfect gas law. Then the following set of equations is obtained:

$$-\sigma\frac{\mathrm{d}}{\mathrm{d}\sigma}\left(\rho\left(R'u_x-\frac{u_r}{\sigma}\right)\right)+\frac{2\rho u_r}{\sigma}=0$$

$$-\sigma\left(R'u_x-\frac{u_r}{\sigma}\right)\frac{\mathrm{d}u_x}{\mathrm{d}\sigma}-R'\frac{\sigma}{\rho}\frac{\mathrm{d}p}{\mathrm{d}\sigma}=0$$

$$-\sigma\left(R'u_x-\frac{u_r}{\sigma}\right)\frac{\mathrm{d}u_r}{\mathrm{d}\sigma}+\frac{1}{\rho}\frac{\mathrm{d}p}{\mathrm{d}\sigma}-\frac{u_\phi^2}{\sigma}=0$$

$$-\sigma\left(R'u_x-\frac{u_r}{\sigma}\right)\frac{\mathrm{d}u_\phi}{\mathrm{d}\sigma}+\frac{u_r u_\phi}{\sigma}=0,\qquad p=\kappa\rho^\gamma \tag{12}$$

The fifth equation is Poisson's relation for the isentropic flow of a calorically perfect gas, which represents the energy equation.

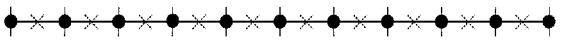

Fig. 5 Schematic of the computational domain for Newton's method: black dots mark grid points, and crosses indicate locations where the equations are imposed.

The appropriate boundary conditions for this problem are (as in the incompressible case) given by $u_r=0$ at $\sigma=0$, and the axial velocity U_e, circumferential velocity V_e, and the pressure P_e are specified at the edge of the core, $\sigma=1$. By defining

$$F=R'u_x-u_r/\sigma \tag{13}$$

combining the azimuthal component of the momentum equations and the continuity equation yields

$$-\sigma F\frac{\mathrm{d}u_\phi}{\mathrm{d}\sigma}+\frac{\sigma}{2}\frac{\mathrm{d}F}{\mathrm{d}\sigma}+\frac{\sigma F}{2\rho}\frac{\mathrm{d}\rho}{\mathrm{d}\sigma}=0\Longrightarrow u_\phi^2=\beta\rho F \tag{14}$$

where β is an arbitrary constant, but such that sign $(\beta)=\mathrm{sign}(\rho F)$. By the use of the axial and radial momentum equation and Eq. (14), the following equation is obtained:

$$R'\beta\rho=-\sigma\frac{\mathrm{d}u_x}{\mathrm{d}\sigma}-R'\sigma^2\frac{\mathrm{d}u_r}{\mathrm{d}\sigma} \tag{15}$$

Combining the continuity, axial momentum equation, the perfect gas law, and Eq. (15) gives

$$\frac{1}{2}\frac{\mathrm{d}}{\mathrm{d}\sigma}\left(u_r^2+u_x^2+u_\phi^2\right)+\kappa\gamma\rho^{\gamma-2}\frac{\mathrm{d}\rho}{\mathrm{d}\sigma}=0 \tag{16}$$

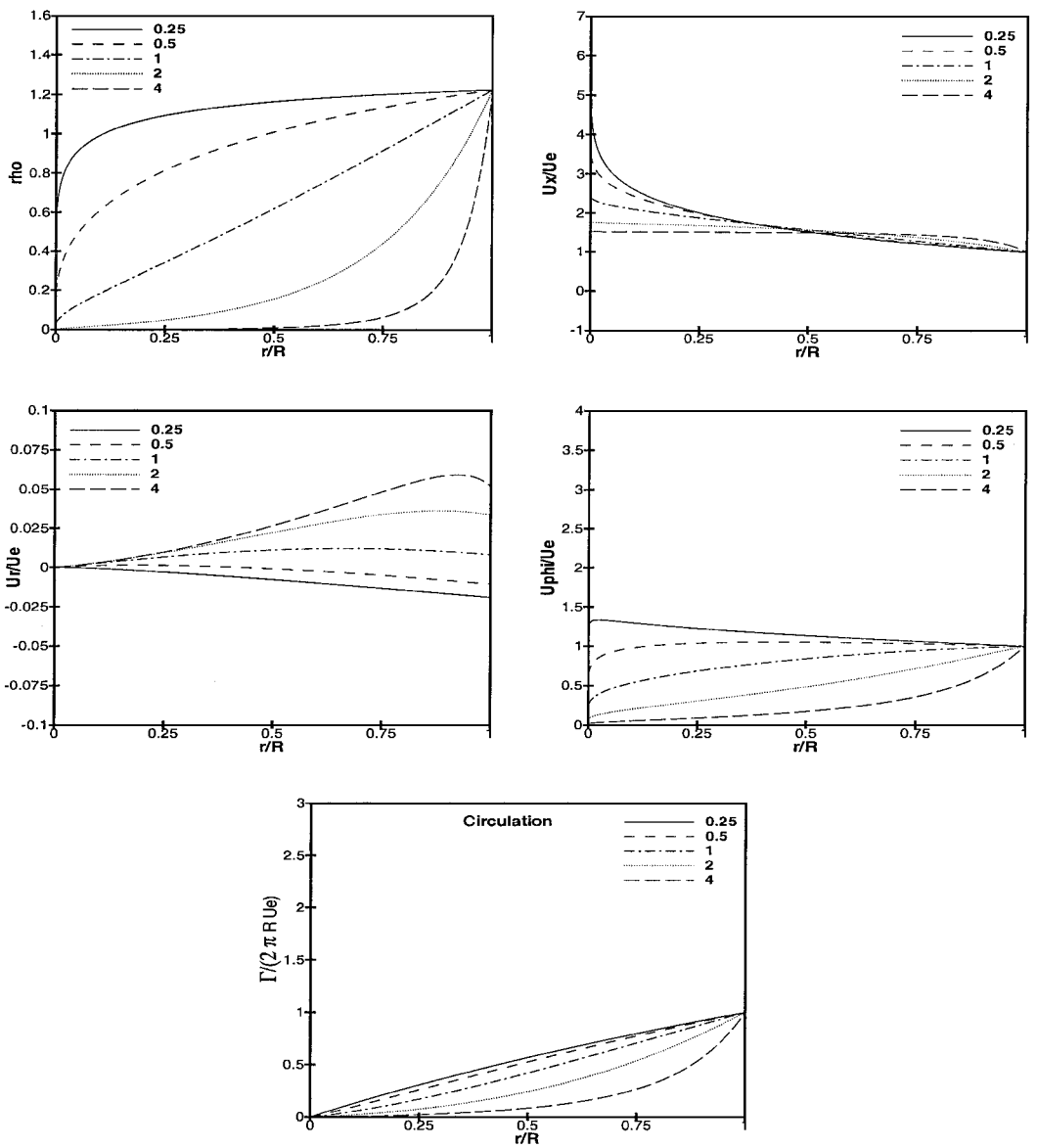

Fig. 6 Compressible jetlike flow solutions for unit swirl number, $R'=0.0625$, and varying Mach numbers 0.25, 0.5, 1, 2, and 4.

This equation can be integrated to yield the condition that the total enthalpy should be constant, that is,

$$\tfrac{1}{2}\left(u_r^2 + u_x^2 + u_\phi^2\right) + [\kappa\gamma/(\gamma-1)]\rho^{\gamma-1} = H_0 \qquad (17)$$

In summary, the following set of equations has been obtained:

$$-\sigma\frac{\mathrm{d}}{\mathrm{d}\sigma}\left(\rho\left(R'u_x - \frac{u_r}{\sigma}\right)\right) + \frac{2\rho u_r}{\sigma} = 0$$

$$-\sigma\frac{\mathrm{d}u_x}{\mathrm{d}\sigma} - R'\sigma^2\frac{\mathrm{d}u_r}{\mathrm{d}\sigma} = R'\beta\rho$$

$$H_0 = \text{const}, \qquad \beta\rho\left(R'u_x - \frac{u_r}{\sigma}\right) = u_\phi^2 \qquad (18)$$

The appropriate boundary conditions are given by $u_x(1) = U_e$, $u_\phi(1) = V_e$, $\rho(1) = \rho_e$, and $u_r(0) = 0$.

This set of equations has already been derived by Brown.[8] To solve this set of equations she assumed that it was possible to neglect the terms $R'\sigma^2(\mathrm{d}u_r/\mathrm{d}\sigma)$ and $\mathrm{d}u_r^2/\mathrm{d}\sigma$ in Eqs. (18) based on the assumption that the vortex core is slender. By the use of this assumption she was able to reduce the system of Eqs. (18) to one differential equation, that is,

$$\rho^{\gamma-1}\left(1 - \frac{\gamma-1}{2}\beta\frac{\mathrm{d}\rho}{\mathrm{d}u_x}\right) = \frac{\gamma-1}{2\kappa\gamma}\left[2H_0 - u_x^2\right] \qquad (19)$$

Subsequently, Brown numerically solved this differential equation and obtained the solution for the three velocity components and the density. In the present study we seek the solution of Eqs. (18) without neglecting terms.

A. Properties of the Solutions

The density, axial, and circumferential component of the velocity have a finite value at the edge of the core. From Eq. (14) it immediately follows that the radial component of the velocity at the edge of the core has a finite value. For $1 < \gamma \leq \frac{5}{3}$, Eq. (17) implies that the velocity components in the interior of the vortex core remain finite. In contrast to the incompressible flow case, a compressible flow solution cannot have a singularity at the axis of the core. At the axis of the core the radial component of the velocity is zero due to the boundary conditions; the other two components of the velocity have a finite value, which might be zero or nonzero. This yields

$$\lim_{\sigma\to 0}\sigma\frac{\mathrm{d}u_r}{\mathrm{d}\sigma} = 0 \qquad (20)$$

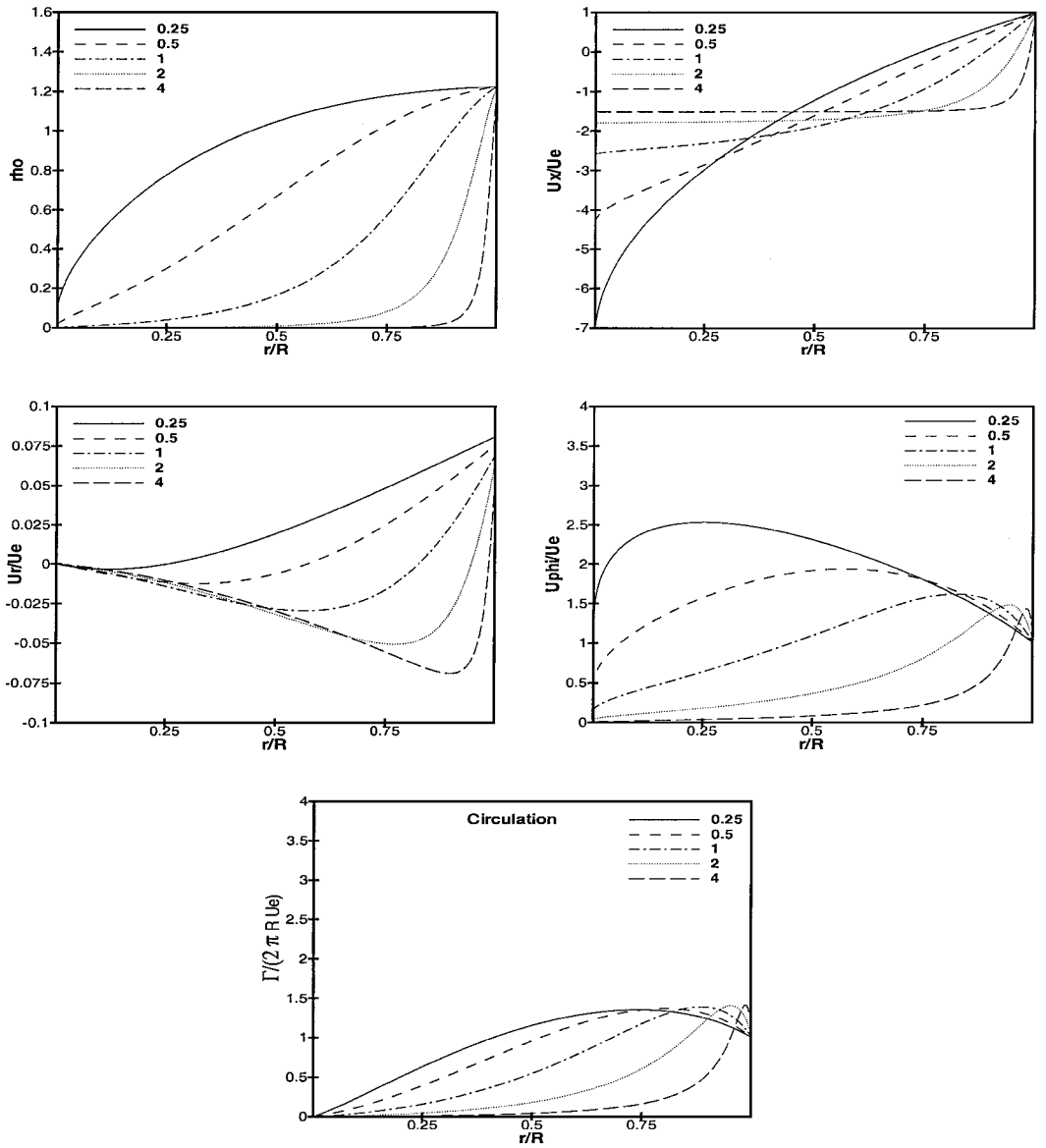

Fig. 7 Compressible wakelike flow solutions for unit swirl, $R' = 0.0625$, and varying Mach numbers 0.25, 0.5, 1, 2, and 4.

$$\lim_{\sigma \to 0} \sigma \frac{du_x}{d\sigma} = 0 \tag{21}$$

$$\lim_{\sigma \to 0} \sigma \frac{du_\phi}{d\sigma} = 0 \tag{22}$$

Using Eq. (15), we get

$$\lim_{\sigma \to 0} \rho = 0 \tag{23}$$

For the compressible flow case the density at the axis of the core is zero, that is, the flow always expands to vacuum at the axis. This immediately implies (through the perfect gas law) that at the axis of the vortex core the pressure is equal to zero. By the combining of the radial component of the momentum equation with the condition

$$\lim_{\sigma \to 0} \sigma \frac{d\rho^{\gamma - 1}}{d\sigma} = 0 \tag{24}$$

which is valid for $\gamma > 1$, it follows that

$$\lim_{\sigma \to 0} u_\phi = 0 \tag{25}$$

that is, the circumferential component of the velocity at the axis of the core becomes zero in the compressible flow case, rather than infinite in the incompressible flow case.

Using Eq. (17) and the information that the radial and circumferential component of the velocity and the density become zero at the axis of the core yields

$$u_x^2(0) = U_e^2 + V_e^2 + u_{rE}^2 + [2\kappa\gamma/(\gamma - 1)](P_e/\kappa)^{1 - 1/\gamma} \tag{26}$$

where u_{rE} is the value of the radial component of the velocity at the edge of the core.

The value of the axial component of the velocity at the axis of the core is finite in compressible form and can be either positive or negative, and for specified U_e, V_e, and P_e, a large range of possible values exists depending on the yet unspecified value of u_{rE}. If, however, one assumes that it is possible to neglect the $du_r^2/d\sigma$ term in Eqs. (18) (as in Ref. 8), the u_{rE} term in Eq. (26) does not appear, and only two possible values for the axial component of the velocity at the axis of the core are obtained. Remarkably, however, Brown[8] excluded the negative value of the axial velocity component at the axis of the vortex core based on the argument that "we intuitively expect a flow in which the vortex is fed by fluid from outside."[8]

B. Numerical Solution Procedure

Equations (18) represent a system of coupled ordinary differential equations in one independent variable. However, the solution of this set of equations has to satisfy boundary conditions at two different values of the independent variable. Therefore, it is not possible to

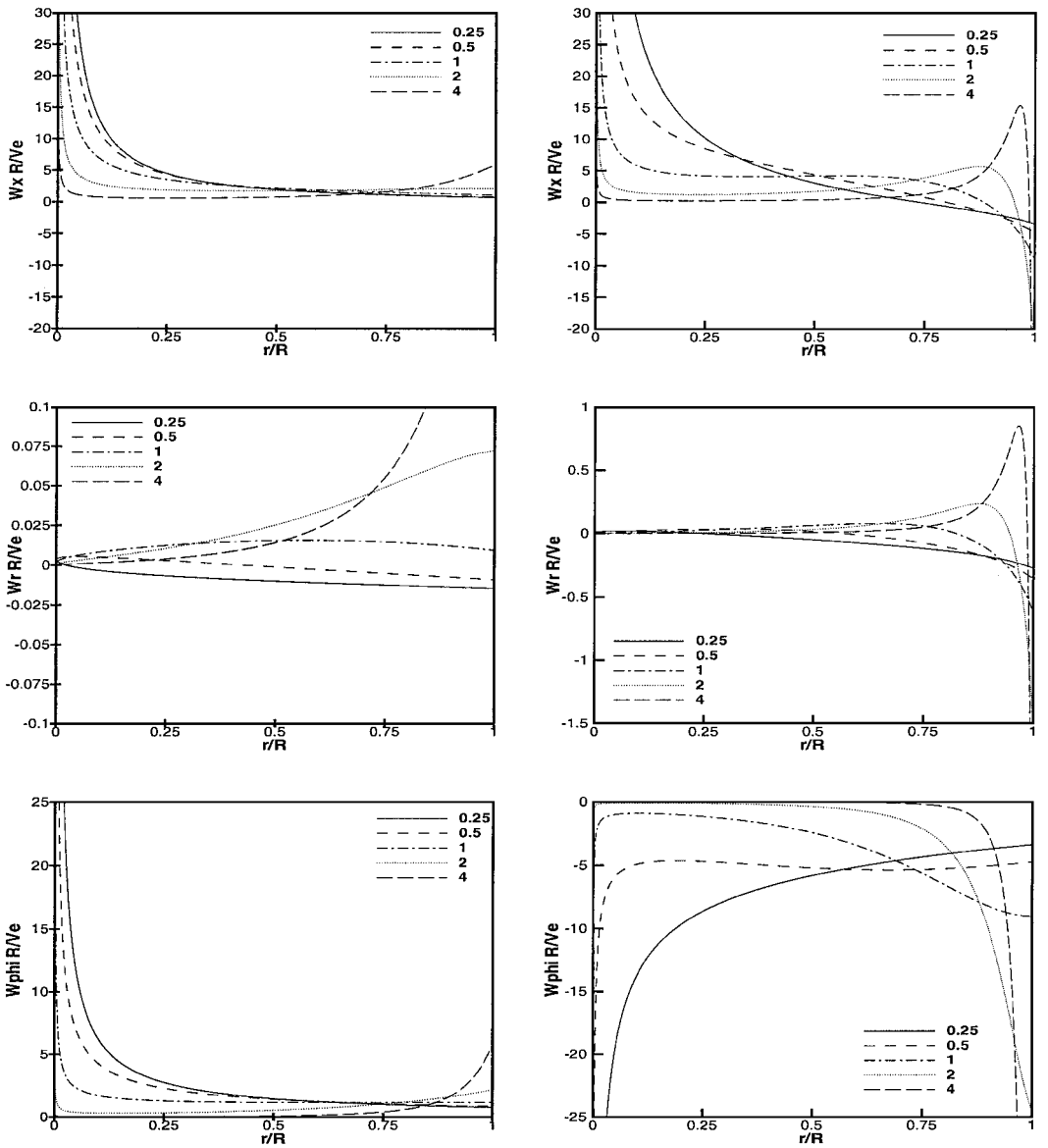

Fig. 8 Vorticity distribution for compressible jetlike (left) and wakelike (right) flow solutions for unit swirl number, $R' = 0.0625$, and varying Mach numbers 0.25, 0.5, 1, 2, and 4.

use a simple marching procedure to obtain the solution of this system of ordinary differential equations. The system of Eqs. (18) can be written as

$$\boldsymbol{E}(\boldsymbol{X}) = \boldsymbol{0} \tag{27}$$

where $\boldsymbol{X}$ is the column vector with the unknowns. The solution of this type of equation can be obtained by a Newton method, that is, given an initial guess $\boldsymbol{X}^n$ an improved solution can be obtained by $\boldsymbol{X}^{n+1} = \boldsymbol{X}^n + \delta\boldsymbol{X}^n$, where $\delta\boldsymbol{X}^n$ is obtained from

$$\left.\frac{\partial \boldsymbol{E}(\boldsymbol{X})}{\partial \boldsymbol{X}}\right|_n \delta\boldsymbol{X}^n = -\boldsymbol{E}(\boldsymbol{X}^n) \tag{28}$$

This process is repeated until the solution ($\boldsymbol{X}^{n+1}$) satisfies Eq. (27) to sufficient order of accuracy. The computational domain (σ runs from 0 to 1) is divided into k equidistant intervals. The edges of these intervals are the locations where the solution will be determined. The midpoints of the intervals are the locations where the equations are imposed. Second-order central differencing is used to evaluate the system of equations in the midpoints. Together with the four boundary conditions this renders a closed problem. In Fig. 5 a schematic of the numerical domain is given.

C. Accuracy Newton Method

To determine the flow solution inside the leading-edge vortex core, the computational domain was divided into 800 equidistant intervals. It was verified that changing the initial condition used in the Newton method resulted in the same converged solution (within machine accuracy). Furthermore, according to Crocco's law [Eq. (10)] for a steady, isoenergetic, isentropic, and inviscid flow not subjected to an external force field, the vorticity vector and velocity vector should be parallel or antiparallel, or equivalently the normalized helicity density [see Eq. (11)] should be either +1 or −1. The numerically obtained solutions for the compressible flow case indeed satisfy these conditions.

D. Results

As for the incompressible flow case, two different solutions are obtained for the flow inside a conical leading-edge vortex core with slope 0.0625 in free air, that is, two distinct solutions are found while keeping the boundary conditions identical. In this section a parameter study is performed to investigate the influence of different parameters on the solution.

1. Varying Mach Number

To demonstrate the influence of compressibility effects on the vortex core, the Mach number at the edge of the vortex core is set

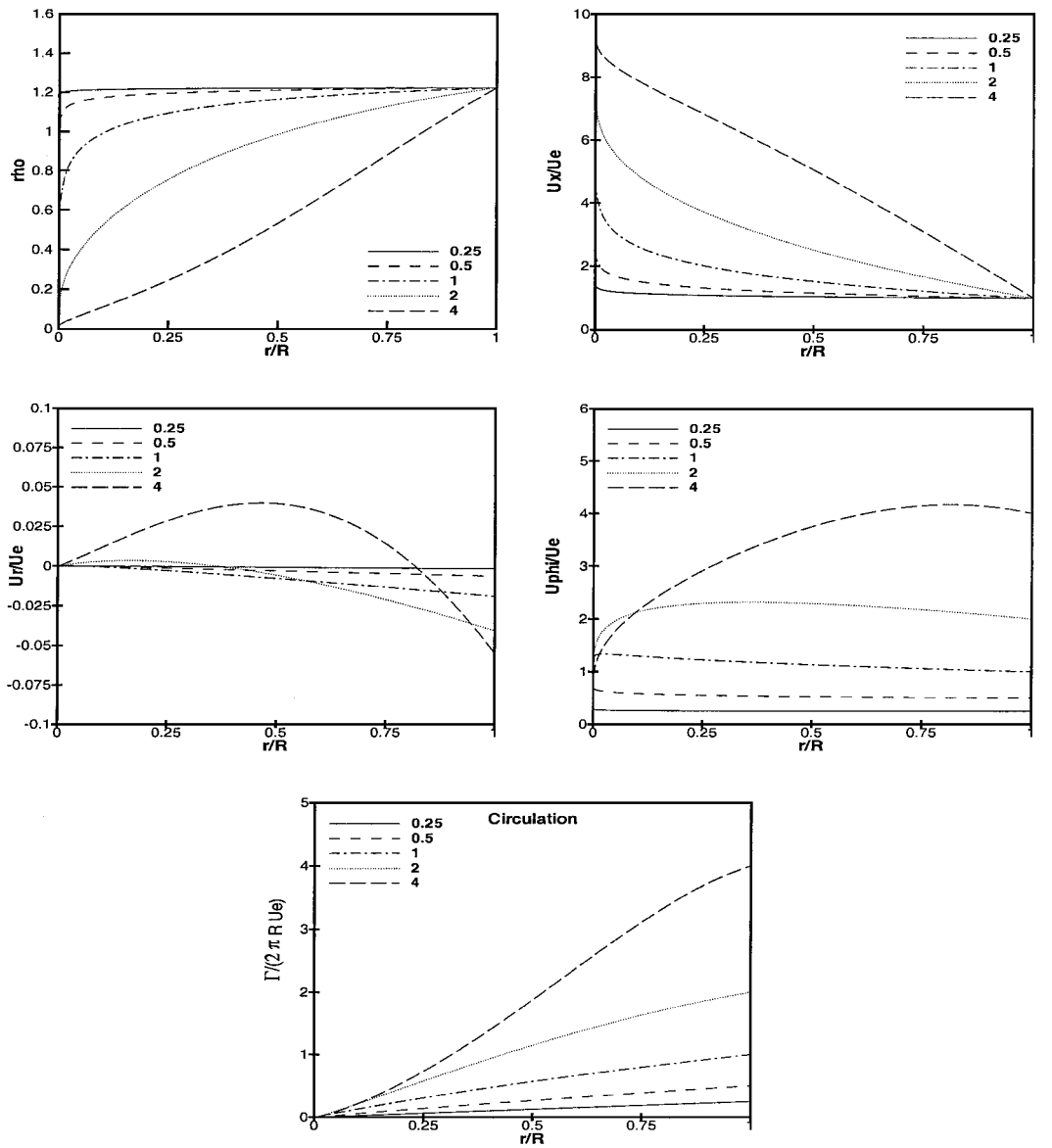

Fig. 9 Compressible jetlike flow solutions for $U_e = \frac{1}{4}$ × (speed of sound) based on freestream values, $R' = 0.0625$, and varying edge swirl (V_e/U_e) numbers 0.25, 0.5, 1, 2, and 4.

to $\frac{1}{4}$, $\frac{1}{2}$, 1, 2, and 4 based on the axial component of the velocity at the edge of the vortex core. The pressure and swirl number at the edge of the core have been kept fixed at $P_e = 10^5$ Pa and $V_e/U_e = 1$, respectively, and the density is set to 1.225 kg/m^3. The results are plotted in Fig. 6 for the first family of solutions and in Fig. 7 for the second family. In Figs. 6 and 7 the velocity components are nondimensionalizedby U_e, and the circulation is scaled by $2\pi RU_e$.

As for the incompressible flow case, two families of solutions are found, one representing a jetlike flow and the second one a wakelike flow. In contrast to the incompressible flow solution, however, where the solution only depends on the swirl number and the slope of the core, the compressible flow solution changes significantly when keeping the swirl and the pressure at the edge constant while varying the axial velocity and therewith the Mach number at the edge of the core.

Jetlike solutions. For the jetlike flow solutions (Fig. 6) increasing the axial velocity at the edge of the core results in an increase in the outer part of the core and a decrease in the inner part of the vortex core of the normalized axial component of the velocity. In accordance with Sec. IV.A, the axial component of the velocity reaches a value of

$$u_x^2(0) = U_e^2 + V_e^2 + u_{rE}^2 + [2\gamma/(\gamma - 1)](P_e/\rho_e) \qquad (29)$$

The radial component of the velocity is much smaller than the other two velocity components. The axial component of the velocity at the axis of the core can, therefore, be estimated by

$$\frac{u_x(0)}{U_e} \approx \left(1 + \frac{V_e^2}{U_e^2} + \frac{2}{(\gamma - 1)M_e^2}\right)^{\frac{1}{2}} \qquad (30)$$

with M_e the Mach number in axial direction at the edge of the vortex core. For the flow in free air presented here with $M_e = 4$, the normalized axial velocity component at the axis is then

$$u_x(0)/U_e \approx 1.5207 \qquad (31)$$

The numerically obtained value is 1.5201, which is in reasonable agreement with the estimate. When increasing the axial velocity at the edge of the core, the density decreases steadily in the interior of the core and always reaches vacuum at the center. The normalized circumferential component of the velocity inside the core decreases with increasing U_e, and in contrast to the incompressible flow case, the circumferential velocity approaches zero as the axis of the core is approached. The radial component of the velocity is relatively small. The velocity component normal to the boundary, that is, $(u_r - R'u_x)/\sqrt{[1 + (R')^2]}$, is negative (inflow) for the jetlike swirling flow solutions. For low Mach numbers, the density and the azimuthal component of the velocity do not appear to tend to zero. However,

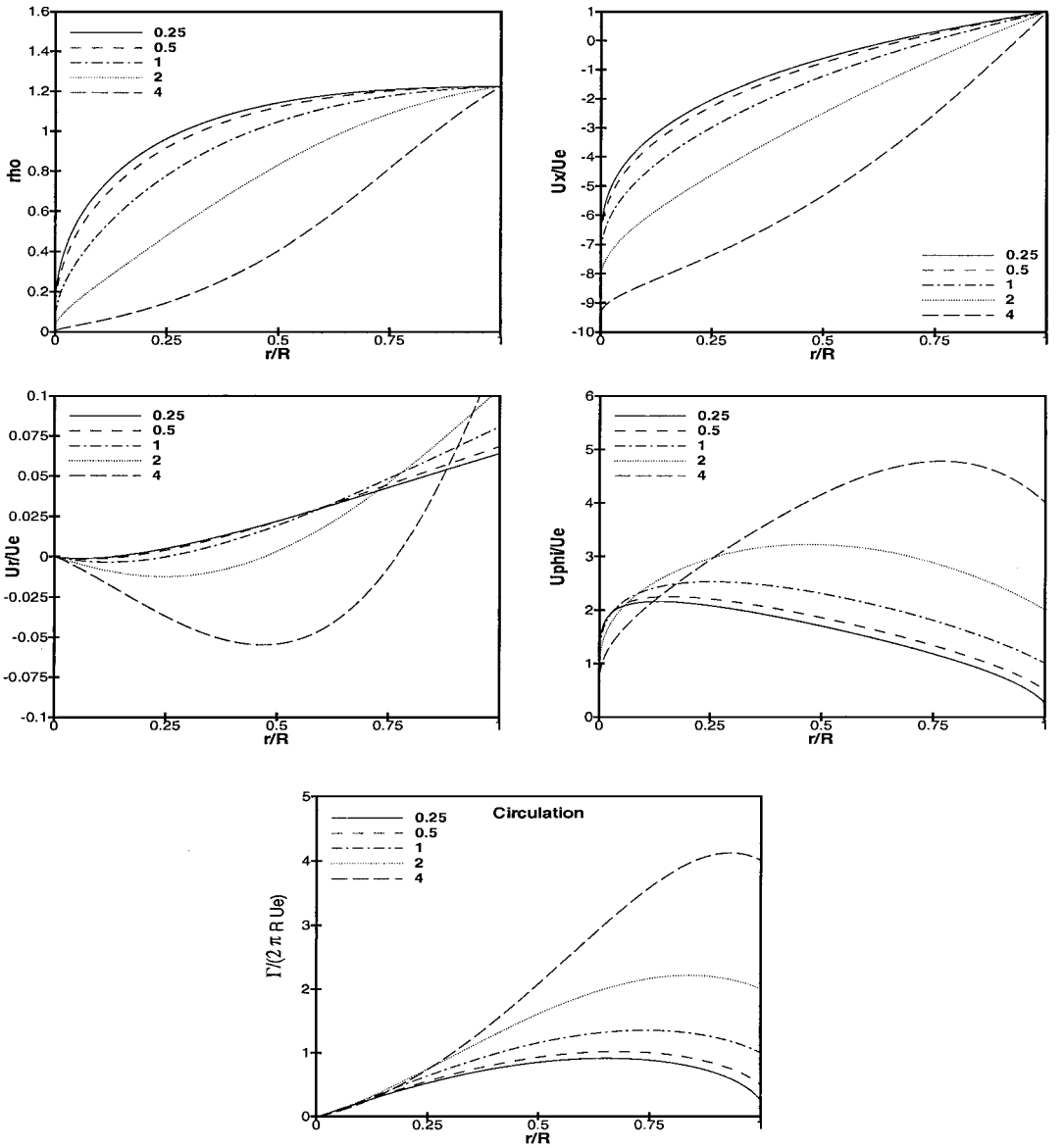

Fig. 10 Compressible wakelike flow solutions for $U_e = \frac{1}{4}$ × (speed of sound) based on freestream values, $R' = 0.0625$, and varying edge swirl (V_e/U_e) numbers 0.25, 0.5, 1, 2, and 4.

the region in which the density and the azimuthal component of the velocity tend to zero for low Mach numbers is apparently limited to a rather small area around the axis of the vortex core. The numerical method employed here is not able to capture this region of the vortex core properly. As a consequence, the axial component of the velocity at the axis of the vortex core is underestimated.

Wakelike solutions. For the wakelike solutions (Fig. 7) a similar type of behavior is found, that is, the normalized axial component of the velocity at the axis increases (becomes less negative) by increasing the edge velocity and reaches a finite value rather than infinity as for the incompressible flow case. With increasing U_e, the density distribution decreases in the interior of the core. Comparison of the two families of solutions for the density distribution shows that the compressibility effect is larger in the wakelike solution, that is, the density distribution in the interior drops faster to low values than for the case of the jetlike solution. Similar to the jetlike solution, the normalized azimuthal component of the velocity decreases by increasing the edge velocity and approaches zero at the axis of the core. Noteworthy in the solutions is that just inside the edge of the core the normalized circumferential velocity component first increases before it starts to decrease. The radial component of the velocity is again an order of magnitude smaller than the other two velocity components. The normal velocity component at the boundary is positive (outflow). These results are in agreement with the analytically obtained properties of the flow solution (see Sec. IV.A).

The vorticity distribution inside the core (see Fig. 8) is similar to that for the incompressible flow case and shows no substantial variation in character when the boundary conditions at the edge of the core are altered. Noteworthy is the region of negative axial vorticity near the boundary for the wakelike solution. As for incompressible flow, the sign of the azimuthal component of the vorticity is different for the two solutions. In Fig. 8, note the different scales for the radial and azimuthal components of the vorticity.

2. *Varying Swirl Number*

Varying the swirl number while keeping the axial velocity at the edge of the vortex core constant results in a similar type of behavior. Figure 9 shows the jetlike solution results when the Mach number at the edge of the core based on the axial velocity component is kept constant at 0.25 and the swirl number is varied. In Fig. 9 (and Fig. 10) the velocity components are nondimensionalized by U_e and the circulation is scaled by $2\pi R U_e$. Increasing the swirl number results in an increase of the normalized axial velocity in the interior of the core and a higher normalized axial velocity at the axis of the core. The azimuthal component of the velocity approaches zero as the distance to the axis of the core becomes smaller. The density

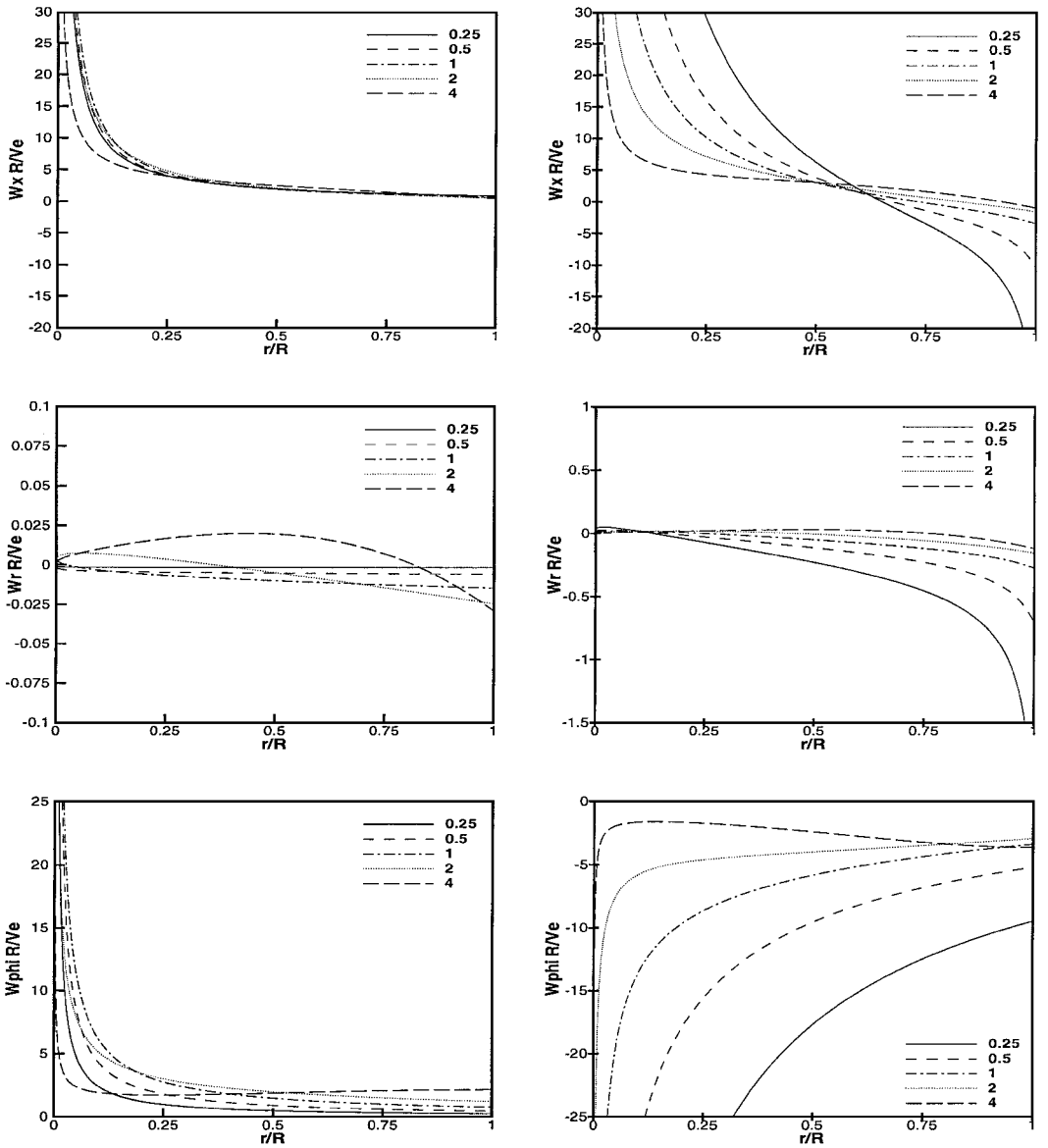

Fig. 11 Vorticity distribution for compressible jetlike (left) and wakelike (right) flow solutions for $U_e = \frac{1}{4}$ × (speed of sound) based on freestream values, $R' = 0.0625$, and varying edge swirl (V_e/U_e) numbers 0.25, 0.5, 1, 2, and 4. Note the different scales for the radial and azimuthal component of the vorticity.

distribution in the interior of the core decays as the swirl number is increased, that is, increasing the swirl number results in a lower density inside the core. As for the incompressible flow case, the flow solution does not change significantly around the unit swirl number, which is believed to be the critical swirl number. For the wakelike solution (Fig. 10) the same type of behavior is observed. Increasing the swirl results in a stronger component of the normalized axial velocity component at the axis of the core. The density distribution in the interior of the core becomes lower with increasing swirl. Again varying the swirl number does not change the general character of the flowfield inside the vortex core significantly. The vorticity distribution inside the core is shown in Fig. 11. The difference in the vorticity distributions between the two types of solutions is again mainly visible in the azimuthal component of the vorticity. Note the different scales for the radial and azimuthal components of the vorticity in Fig. 11.

The presence of two different families of flow solutions satisfying identical boundary conditions for the flow inside the leading-edge vortex core has a parallel with the existence of the two families of similarity solutions of the two-dimensional boundary-layer equations for the flow with a pressure gradient, though it is emphasized that the two problems are not related to each other. Assuming similarity solutions for the velocity distribution results in the Falkner–Skan equation.[18] The resulting two-point boundary-value problem has two families of solutions for specific boundary conditions, that is, a convential boundary-layer solution and a solution with reversed flow close to the surface. In the present investigation also, two different families of solutions have been obtained for identical boundary conditions. Remarkably, however, both families of flow solutions exist for all boundary conditions considered, whereas for the Falkner–Skan equation a reversed flow solution is only obtained in the case where an adverse pressure gradient is present along the outer edge of the boundary layer.

In recent publications (e.g., Refs. 16 and 17), a switch in the sign of the azimuthal vorticity component has been identified as a key element in the vortex breakdown process. The existence of multiple flow solutions satisfying identical boundary conditions where the azimuthal component of the vorticity has changed direction might indicate that vortex breakdown could be a jump between two steady-state flow solutions, which, at least for its onset, could already be present in the inviscid Euler equations. To substantiate this issue, however, it will be necessary to consider the stability of both families of flow solutions. It might be possible that the stability characteristics of both families of flow solutions strongly depend on parameters such as the Mach number or the swirl number, as for the jetlike flow solutions that have been obtained for swirl numbers far exceeding the values formed in experiments. Furthermore, following the work of Mayer and Powell[9] it is also necessary to investigate the influence of viscosity on the flow solutions in the interior of the vortex core.

V. Conclusions

Experimental observations of the flowfield inside the vortex formed at the leading edge of a highly swept wing at an angle of attack indicate that the leading-edge vortex consists of a fairly axisymmetric, compact, and slender region of concentrated vorticity that grows linearly in downstream direction. This region of high vorticity seems to consist of an inviscid rotational outer core and a viscid subcore. Experimental observations indicate that, at least for the initial part of the leading-edge vortex core, the flowfield inside the vortex core is nearly conical. Based on these observations, Hoeijmakers[10] derived two families of conical similarity flow solutions of the incompressible and axisymmetric form of the Euler equations satisfying identical boundary conditions to describe the flowfield inside an isolated leading-edge vortex core. One family of flow solutions represents jetlike swirling flow solutions, which have earlier also been obtained by Hall[5] and Ludwieg[6] for slender vortex cores. For the outer part of the vortex core, this flow solution resembles the flowfield inside a leading-edge vortex. The second family of flow solutions represents wakelike swirling flow solutions. At the axis of the vortex core, however, these solutions possess a logarithmic singularity in the axial and azimuthal components of the velocity as well as in the pressure. This logarithmic singularity at the axis of the vortex core is of course nonphysical and is due to the neglect of compressibility and viscosity effects in the solution. Considering the flow solutions in more detail reveals that the velocity component normal to the edge of the vortex is negative (inflow) for jetlike swirling flows and positive (outflow) for wakelike swirling flows. Furthermore, the azimuthal component of the vorticity differs in direction for the two flow solutions. For jetlike swirling flows, the velocity and vorticity vector are parallel, whereas for wakelike swirling flows, they are antiparallel.

In the present study, conical similarity flow solutions for the compressible and axisymmetric form of the Euler equations, thereby still neglecting the influence of viscosity, are obtained. Analysis of the resulting equations shows that the azimuthal component of the velocity and the density approach zero as the axis of the vortex core is approached, whereas the axial component of the velocity attains a finite value at the axis of the core. Adding the effect of compressibility to Hall's[5] solution results in removing the logarithmic singularity in the axial and azimuthal components of the velocity. However, at the axis of the vortex core, the solution reaches vacuum conditions. In a real flow, viscosity might have a significant effect on the flow solution near the axis of the vortex core, and vacuum conditions may not be reached at the axis of the vortex core. Analysis of the resulting equations indicates that multiple flow solutions satisfying identical boundary conditions are possible.

Two different families of flow solutions have been numerically obtained. The first family of flow solutions represents jetlike swirling flow solutions. For the outer part of the vortex, the solution of the flowfield qualitatively resembles the flow inside a leading-edge vortex core before breakdown. This family of solutions has already been obtained by Brown[8] for slender vortices. The second family of solutions represents a completely new family of solutions, which have a wakelike character. Considering the flow solutions in more detail reveals that the normal component of the velocity at the edge of the vortex core is negative (inflow) for jetlike swirling flows and positive (outflow) for wakelike swirling flows. These results are in line with the results already obtained for the incompressible flow case. Similar to the incompressible flow case, the velocity and vorticity vector are coparallel for jetlike swirling flows and antiparallel for wakelike swirling flows. Furthermore, the azimuthal component of the vorticity has a different sign for the two flow solutions. Varying the boundary conditions at the edge of the vortex core does not change the character of the density and velocity distributions inside the leading-edge vortex significantly. In particular, varying the swirl number at the edge of the vortex core does not change the character of the obtained flow solution.

References

[1]Earnshaw, P. B., "An Experimental Investigation of the Structure of a Leading-Edge Vortex," Aeronautics Research Council, Rept. 22.876, London, 1961.

[2]Verhaagen, N., and van Ransbeeck, P., "Experimental and Numerical Investigation of the Flow in the Core of a Leading-Edge Vortex," AIAA Paper 90-0384, Jan. 1990.

[3]Visbal, M. R., "Computational and Physical Aspects of Vortex Breakdown on Delta Wings," AIAA Paper 95-0585, Jan. 1995.

[4]Visser, K. D., and Nelson, R. C., "Measurements of Circulation and Vorticity in the Leading-Edge Vortex of a Delta Wing," *AIAA Journal*, Vol. 31, No. 1, 1994, pp. 104–111.

[5]Hall, M. G., "A Theory for the Core of a Leading-Edge Vortex," *Journal of Fluid Mechanics*, Vol. 11, 1961, pp. 209–224.

[6]Ludwieg, H., "Zur Erklärung der Instabilität der über Angestellten Deltaflügeln auftretenden Freien Wirbelkerne," *Zeitschrift für Flugwissenschaften*, Vol. 10, No. 6, 1962, pp. 242–249.

[7]Stewartson, K., and Hall, M. G., "The Inner Viscous Solution for the Core of a Leading-Edge Vortex," *Journal of Fluid Mechanics*, Vol. 15, 1963, pp. 306–318.

[8]Brown, S. N., "The Compressible Leading-Edge Vortex," *Journal of Fluid Mechanics*, Vol. 22, 1965, pp. 17–32.

[9]Mayer, E. W., and Powell, K. G., "Similarity Solutions for Viscous Vortex Cores," *Journal of Fluid Mechanics*, Vol. 238, 1992, pp. 487–507.

[10]Hoeijmakers, H. W. M., "Aspects of Modelling and Numerical Simulation of Leading-Edge Vortex Flow," *Proceedings of IUTAM Symposium Fluid Dynamics of High Angle of Attack*, edited by R. Kawamura and Y. Aihara, Springer–Verlag, Berlin, 1992, pp. 199–210.

[11]Benjamin, T. B., "Theory of the Vortex Breakdown Phenomenon," *Journal of Fluid Mechanics*, Vol. 14, 1962, pp. 593–629.

[12]Wang, S., and Rusak, Z., "The Dynamics of a Swirling Flow in a Pipe and Transition to Axisymmetric Vortex Breakdown," *Journal of Fluid Mechanics*, Vol. 340, 1997, pp. 177–223.

[13]Berger, S. A., and Erlebacher, G., "Vortex Breakdown Incipience: Theoretical Considerations," *Physics of Fluids*, Vol. 7, No. 5, 1995, pp. 972–982.

[14]Verhaagen, N. G., Meeder, J. P., and Verhelst, J. M., "Boundary Layer Effects on the Flow of a Leading-Edge Vortex," AIAA Paper 93-3463, Aug. 1993.

[15]Verhaagen, N. G., Houtman, E. M., and Verhelst, J. M., "A Study of Wall Effect on the Flow of a Delta Wing," AIAA Paper 96-2389, June 1996.

[16]Brown, G. L., and Lopez, J. M., "Axisymmetric Vortex Breakdown Part 2: Physical Mechanisms," *Journal of Fluid Mechanics*, Vol. 221, 1990, pp. 553–576.

[17]Darmofal, D. L., "The Role of Vorticity Dynamics in Vortex Breakdown," AIAA Paper 93-3036, July 1993.

[18]Young, A. D., *Boundary Layers*, BSP Professional Books, Oxford, 1989, pp. 73–79; also published in AIAA Education Series, AIAA, Washington, DC, 1989.

J. R. Bellan
Associate Editor